Structural Engineering and Mechanics, *Vol. 61, No. 1 (2017) 77-90*
DOI: https://doi.org/10.12989/sem.2017.61.1.077

Seismic assessment and finite element modelling of glazed curtain walls

Nicola Caterino*[1,3], Marta Del Zoppo[1], Giuseppe Maddaloni[2,3], Antonio Bonati[3], Giovanni Cavanna[3] and Antonio Occhiuzzi[1,3]

[1]*Department of Engineering, University of Naples "Parthenope", Naples, Italy*
[2]*Department of Engineering, University of Benevento "Sannio", Benevento, Italy*
[3]*Construction Technologies Institute, Italian National Research Council (CNR), San Giuliano Milanese, Milan, Italy*

(Received March 4, 2016, Revised July 14, 2016, Accepted July 19, 2016)

Abstract. Glazed curtain walls are façade systems frequently chosen in modern architecture for mid and high-rise buildings. From recent earthquakes surveys it is observed the large occurrence of non-structural components failure, such as storefronts and curtain walls, which causes sensitive economic losses and represents an hazard for occupants and pedestrians safety. In the present study, the behavior of curtain wall stick systems under seismic actions has been investigated through experimental in-plane racking tests conducted at the laboratory of the Construction Technologies Institute (ITC) of the Italian National Research Council (CNR) on two full-scale aluminium/glass curtain wall test units. A finite element model has been calibrated according to experimental results in order to simulate the behavior of such components under seismic excitation. The numerical model investigates the influence of the interaction between glass panels and aluminium frame, the gasket friction and the stiffness degradation of aluminium-to-glass connections due to the high deformation level on the curtain walls behavior. This study aims to give a practical support to researchers and/or professionals who intend to numerically predict the lateral behavior of similar façade systems, so as to avoid or reduce the need of performing expensive experimental tests.

Keywords: non-structural elements; curtain walls; stick-wall systems; seismic behavior; in-plane test

1. Introduction

During the last years, the interest on the behaviour of non-structural elements during seismic events raised significantly. Recent earthquakes have shown frequent damages to non-structural components, so as claddings and glazed facades, and attested that the higher costs of reparation are related to architectural parts. Therefore, the need of developing reliable methods for preventing economic and human losses is confirmed. In particular, the large use of glazed curtain wall systems as external enclosures pushed the researchers to investigate the response of such non-structural elements when an earthquake occurs.

The glazing curtain walls are non-structural façade components, often covering more than one storey, thoroughly hung to the principal structure by means of connections at the beam/slab level. The damage of such components during earthquakes causes sensitive economic losses and hazard for pedestrians and occupants safety. The in-plane behaviour of curtain walls strictly depends by that of the principal structure, whereas the out-of-plane behaviour is further controlled by the wind action. Post-earthquake surveys (Evans, Kennett *et al.* 1988, Filiatrault, Christopoulos *et al.* 2002, Hosseini 2005, Baird, Palermo *et al.* 2011) confirmed the principal cause of curtain walls damages is the in-plane displacement rate caused by the supporting structure movements, more than the acceleration demand for the curtain wall itself. When the principal structure is subjected to seismic actions, it develops relative displacements between consecutive storeys (i.e., interstorey drift). Since the external glazing systems are connected to the structure's beams/slabs, the interstorey drifts cause damages to the curtain wall systems up to the glass panels cracking and/or fall-out.

First experimental studies have been conducted on the in-plane behavior of window glass panels under static in-plane loads, investigating the glass deformation related to the horizontal drift (Bouwkamp and Meehan 1960, Bouwkamp 1961). The mechanical behavior of structural glass panels has been also investigated, characterizing the response of monolithic and laminated structural glass annealed (Behr, Minor *et al.* 1993) and tempered (Carré and Daudeville 1999), also varying boundary conditions having influence on the glass mechanical properties (e.g., temperature).

Several experimental in-plane tests have been performed on full-size single glass test units with aluminium framed mullions/transoms (Lim and King 1991, Thurston and King 1992, Pantelides and Behr 1994, Behr, Belarbi *et al.* 1995a, Behr, Belarbi *et al.* 1995b, Sucuoğlu and Vallabhan 1997, Behr 1998), with different structural glass typologies, clearance values and anchorage systems (i.e., sealant distribution and properties). The tests confirmed that the response under monotonic loads is the same achieved during load-reversal tests. Common mechanisms of damage recognised are gaskets dislodging, glass crushing at corners, glass cracking and glass panels fall-out. Moreover, it has

*Corresponding author, Assistant Professor
E-mail: nicola.caterino@uniparthenope.it

ISSN: 1225-4568 (Print), 1598-6217 (Online)

Table 1 Worldwide codes dealing with seismic design and verification of glazed curtain walls

Region	Code	Seismic capacity?	Seismic demand?
USA	AAMA 501.6 (2001)	Yes: definition of a testing procedure	No
USA	FEMA 450 (2003)	No	Yes, in terms of drift
USA	ASCE 7-10 (2013)	No	Yes, in terms of drift
Japan	JASS 14 (1996)	No	Yes, in terms of drift
Europe	UNI EN 13830 (2015)	Yes: definition of a testing procedure	No

been observed that the glass plates can cause significant plastic deformations of the aluminium frame where the contact happens (Behr, Belarbi *et al.* 1995a). Bi-directional experimental tests have also been performed on plane (Thurston and King 1992) and corner configurations (i.e., "*L*" shaped units) (Behr, Belarbi *et al.* 1995b), in order to observe both the in-plane and out-of-plane response. Both curtain walls with monolithic and laminated glass panels have been examined and compared by Thurston and King (1992), Pantelides and Behr (1994), Behr (1998). The drift capacity and stress distribution of a single glass panel into a steel frame subjected to in-plane load have also been studied by Huveners (2007) for different glass-to-frame joint configurations.

The load protocol widely used for experimental in-plane tests is the so called "crescendo test" (Pantelides, Truman *et al.* 1996). It is characterized by monotonically increasing amplitude and sinusoidal drift cycles. It is generally used to determine the serviceability drift limits and ultimate drift limits for architectural glass components subjected to cyclic in-plane racking displacements. However, other load protocols have also been adopted in experimental tests on curtain walls systems (Hutchinson, Zhang *et al.* 2011).

Several authors proposed strategies for improving the in-plane response of curtain walls systems. Tests on earthquake-isolated glazing systems (Brueggeman, Behr *et al.* 2000) demonstrated better performances both in terms of serviceability and ultimate response (i.e., glass fall-out). In order to reduce the damage of glass panels, PET films have been often applied on the external layer of glass (Thurston and King 1992, Memari, Behr *et al.* 2004, Hutchinson, Zhang *et al.* 2011). Moreover, since the glass panels crush-crack is generally concentrated at the corners, experimental tests have been carried out on glass panels with rounded corners (Memari, Kremer *et al.* 2006).

Fragility curves for glazing systems in terms of probability and possible consequence of damages as a function of the drift have been presented by O'Brien, Memari *et al.* (2012), on the basis of experimental in-plane racking tests reported in literature.

However, a lack of analytical formulations able to predict the drift capacity of glazed systems has been recognised. Bouwkamp and Meehan (1960) observed that displacements of glass panels subjected to in-plane loads can be seen as the sum of two components: rigid body rotation, until the contact between glass panel and frame, and diagonal compressive deformation after the contact happens. Based on this assumption, an analytical formulation for the drift capacity of glass frames has been proposed by Sucuoğlu and Vallabhan (1997). An application of the analytic procedure for the evaluation of seismic demand and drift capacity has been reported by Sivanerupan, Wilson *et al.* (2009).

A simple relation for the prediction of ultimate drift capacity of full-size glazed curtain walls based on the failure load of a small-size glass panels has been suggested by Memari, Behr *et al.* (2000), in order to avoid expensive full-size tests. For the evaluation of the cracking drift for existing glazed curtain walls, a seismic rating system has been proposed by Memari and Shirazi (2004). According to this procedure, a score is assigned at each curtain wall, based on geometric and mechanical properties and on the seismic drift demand.

In order to make general predictions on the behaviour of new and existing glazed curtain wall systems and, in particular, on the drift at glass cracking and fall-out during seismic actions, a finite element model has been developed by Memari, Shirazi *et al.* (2007, 2011) and a calibration on experimental results has been proposed.

The present research focuses on stick wall systems. First, it describes a review of worldwide technical codes provisions about the seismic performance of glazed curtain walls. Then, the results of experimental tests on two full-scale aluminium/glass curtain wall test units are presented. Finally, a finite element model for the analysed façades, developed within the software SAP2000 environment (2014) and aiming at reproducing the above experimental results is described. The corresponding numerical simulations allowed to clearly highlight the role that the non-linear interaction between glass and aluminium plays in defining the strength and the stiffness of the composite system during a stepwise incremental load activity. The discussion of the results should assist researchers and/or professionals in numerically predicting the lateral behavior of similar façade systems, so as to avoid or reduce the need of performing expensive experimental tests.

2. Overview of seismic codes provisions for glazed curtain walls

Glazed curtain walls levels of performance during earthquakes are divided, as usual in structural engineering, in serviceability and ultimate limit states. In conventional design of external glazing systems, the air and water permeability during the reference life should be guaranteed (serviceability limit state) and the glass fall-out during strong earthquakes should be avoided (ultimate limit state). As aforementioned, the horizontal relative displacements represent the main cause of damages for façade systems as

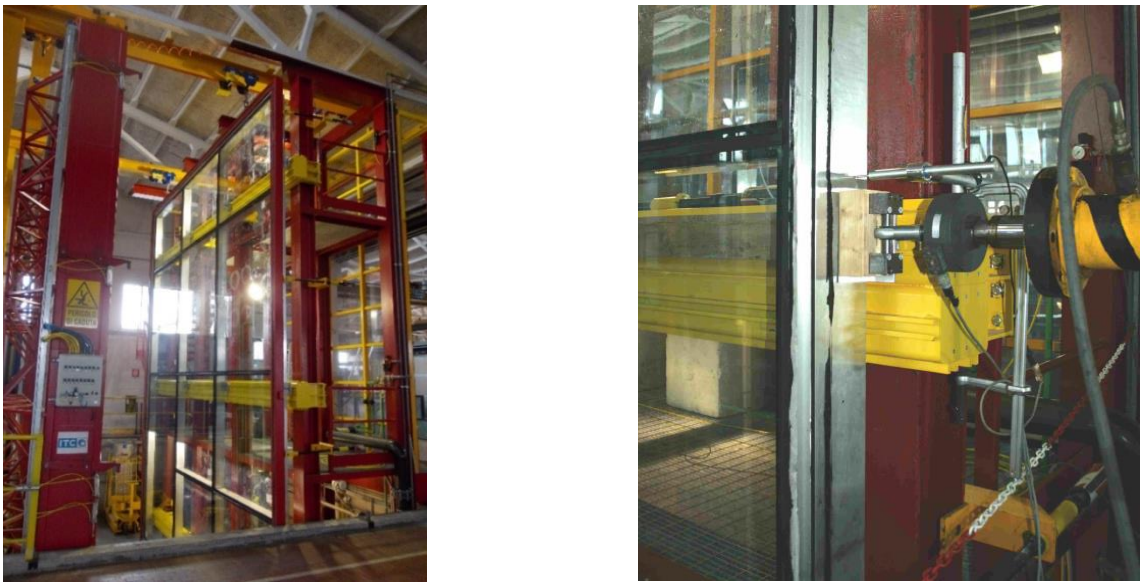

(a) (b)

Fig. 1 Test set-up (a) and lateral load application by means of a hydraulic jack (b)

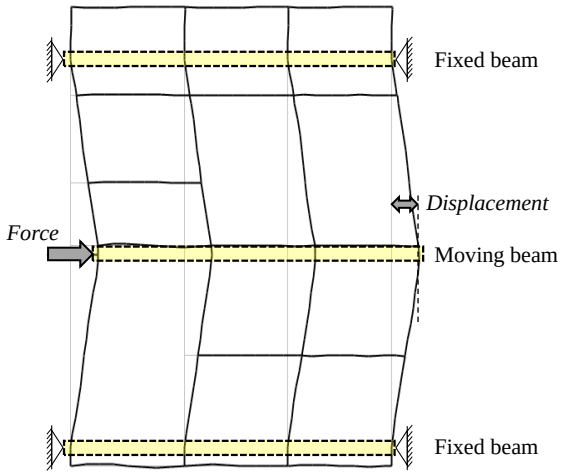

Fig. 2 Schematic representation of the setup: moving and fixed beams, point of application of the lateral force, displacement of the mid-height beam

curtain walls. Current codes provide specific limitations to the interstorey drift D_p referred to the structural frame, in order to avoid damages to non-structural components, like partition walls and claddings. However, a lack of specific prescriptions about the verification of glazed curtain walls is recognised.

Eurocode 8 (2003) gives general prescriptions for the design of non-structural elements, even if without specific reference to curtain walls systems. According to the force-based approach, the code provides the equivalent seismic force to be used to design and check generic non-structural components. Among worldwide codes, those that specifically refer to glazed curtain walls are those reported in Table 1, although each of these concerns separately the seismic demand or seismic capacity.

The American codes FEMA 450 (2003) and ASCE 7-10 (2013) also provide the seismic design force for architectural components, with explicit reference to exterior non-structural wall elements. According to such codes, glazed curtain walls should also be able to accommodate the seismic relative displacements D_p of the structure for the selected limit state. They provide the minimum value for the drift capacity of the glazing systems ($\Delta_{fallout}$) reported in Eq. (1), where I is an importance factor.

$$\Delta_{fallout} \geq 1.25 I D_p \geq 13mm \tag{1}$$

The value of $\Delta_{fallout}$ can be evaluated with experimental dynamic racking tests, as indicated in specific regulations by the American Architectural Manufacturers Association (AAMA 501.6 2001), or through specific numerical analyses. According to ASCE 7-10 (2013), the evaluation of $\Delta_{fallout}$ can be avoided when the drift Δ_{clear} that causes the initial glass-to-frame contact is higher than 1.25 D_p. The value of Δ_{clear} can be assessed according to Eq. (2), where h and b are the glass panel width and height respectively, and c is the average clearance between the glass edges and the frame. This expression for Δ_{clear} provided by the above regulations comes from the researches of Bouwkamp and Meehan (1960) and Sucuoğlu and Vallabhan (1997).

$$\Delta_{clear} = 2c\left(1+\frac{h}{b}\right) \geq 1.25 D_p \tag{2}$$

Similarly, the Japanese Code (JASS 14 1996) specifically identifies a minimum value of drift capacity for the seismic verification of glazing systems for different earthquakes intensities as a function of the interstorey height referred to the building. In particular, for severe earthquakes, the glazed systems should be designed for a relative displacement of 1% of the interstorey height.

The present work is intended to lay the basis to understand how the above drift limits are related to the actual damaging of glass façade and eventually how the

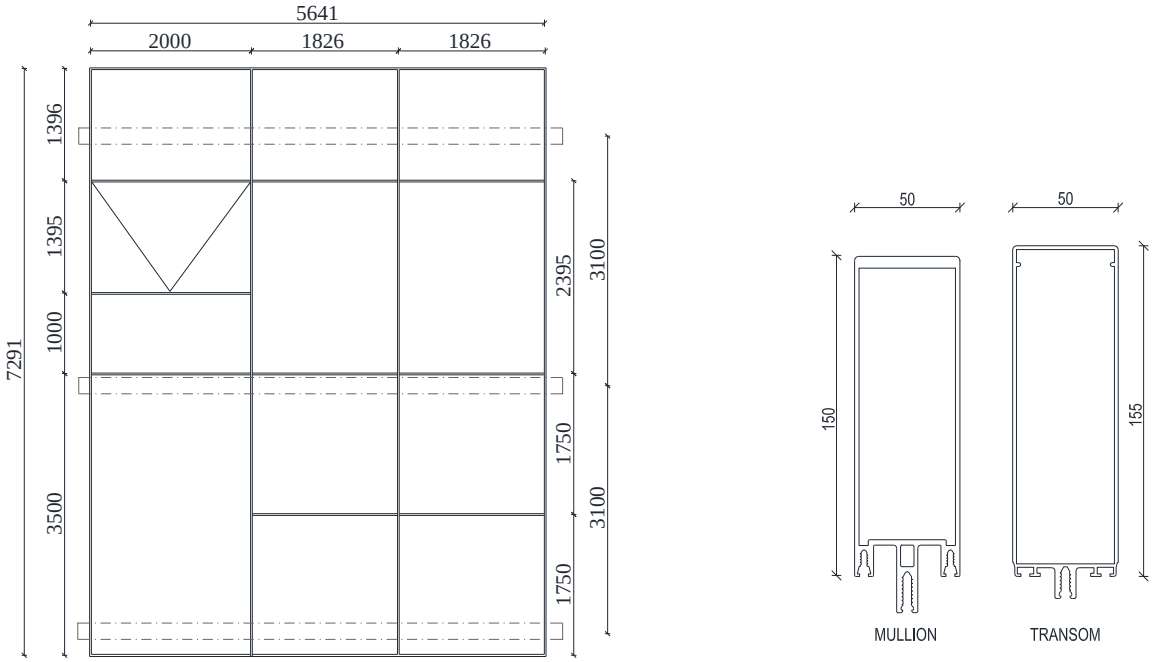

(a) (b)

Fig. 3 Façade A: geometry (a) and transom/mullion cross-sections (b), dimensions in mm

code approaches could be improved or changed when dealing with the seismic evaluation of such architectural components.

3. Experimental assessment of seismic lateral behaviour for two commercial stick curtain walls

The seismic behaviour of two full-scale stick curtain walls has been experimentally evaluated by performing full-size in-plane tests at the laboratory of the Construction Technologies Institute (ITC) of the Italian National Research Council (CNR). The two types of stick curtain walls tested are actually produced and available on the market, and are both mainly made of an aluminium transom-mullion frame and insulated glazing systems. They were chosen as mainstream products in the European market of stick curtain walls, designed without any care to seismic actions.

In the following, first the experimental setup and instrumentation are introduced, then the activity and results for each of the two façades are presented and discussed. The two specimens are referred to as "façade A" and "façade B".

3.1 Experimental setup and equipment

The test facility consists in a steel frame 5,72×7,37 m with three rigid beams, which simulate the principal structure's beams or slabs (Fig. 1(a)). The beams can be installed at different heights to adapt different configurations of curtain walls. They can be moved in the horizontal direction to simulate seismic induced lateral displacements. For the specific tests herein described, only the intermediate steel beam has been pushed in the horizontal direction, while the upper and lower beams were firmly fixed to the external frame (Fig. 2).

The mullions of the full-scale test units have been rigidly connected to the steel beams. Force control tests have been performed pushing over, in the horizontal in-plane direction, the external mullion, in correspondence of the mullion-beam connection (Fig. 1(b)), by means of an hydraulic jack (General Hydraulic, stroke ±600 mm, maximum load 200 kN) connected to an external rigid reaction system. A 50 kN LeBow load cell has been used to measure the force applied by the actuator. Two linear potentiometric displacement transducers (i.e., LVDT), having range ±100 mm, have been placed on the two external mullions, along the axis of the actuator, to measure horizontal displacements of the central rigid horizontal beam. A 10 Hz continuous data acquisition has been performed for load and displacement data during the tests.

3.2 Façade A: description of the specimen, experimental activity and results

The first façade tested covers two storeys (7,300 mm height and 5,650 mm width), with 3,100 mm interstorey height. The test unit is characterized by four mullions and four transoms (see Fig. 3(a)). Extruded aluminium profiles are used for mullions and transoms and their cross-sections are shown in (Fig. 3(b)). All mullions have same cross-section, so as the transoms. The insulated glazing units are made with fully tempered glass panels, thickness 8+16+8 mm, linearly supported on the edges trough silicone gaskets. A single openable window is present in this specimen, whereas the other glass panels are fixed.

The mullions are continuous along the entire façade

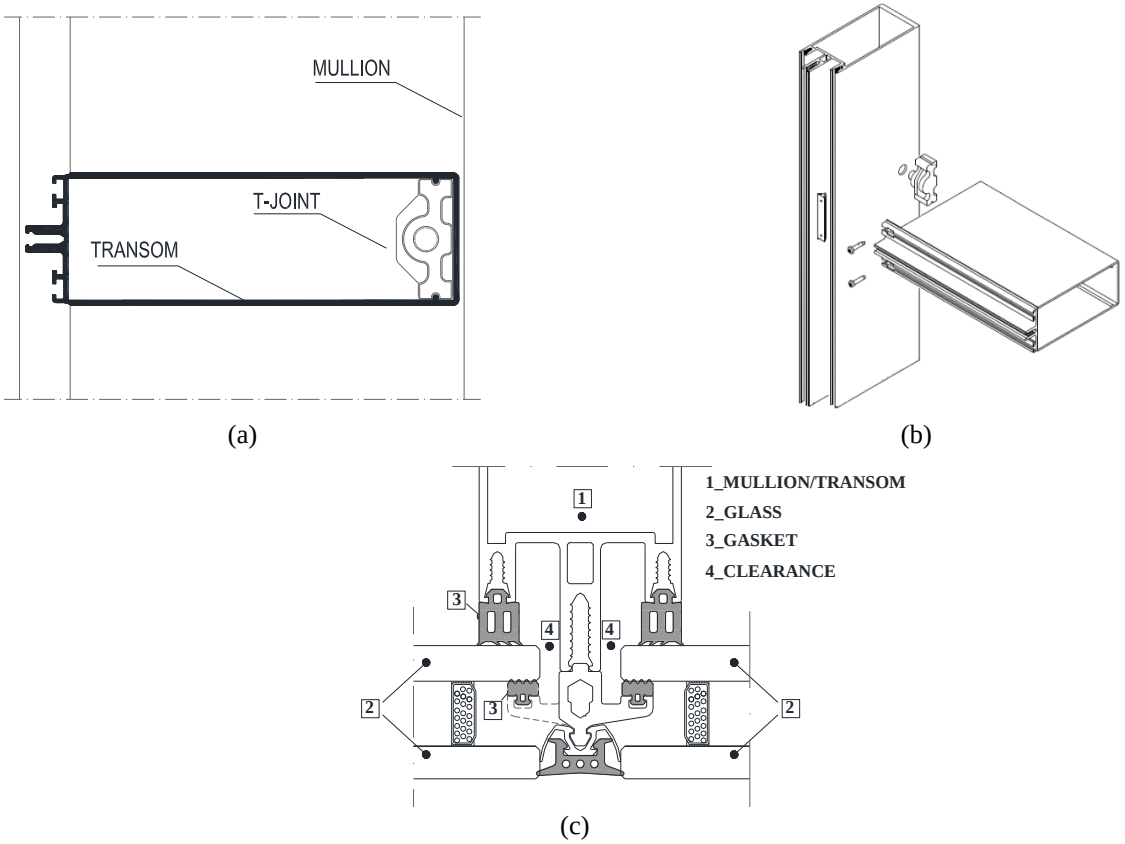

Fig. 4 Façade A: Transom-to-mullion connection 2d (a) and 3d provided by the manufacturer (b), glass-to-frame connection (c)

height, whereas the transoms are supported between the mullions.

The transom-to-mullion connection is realized with two steel screws which connect directly the transom to the mullion and a special "T-joint" for transom, see Fig. 4(a). The steel screws connect the transom to the mullion by a special L-shaped plate joined with the mullion. The "T-joint" connects the mullions to the transom by a trigger button which makes, together with the screws, the overall connection to be very stiff regards relative displacements as well as relative rotation between connected elements (Fig. 4(b)).

The glass-to-frame connection is obtained adopting silicone gaskets distributed along the glass panels edges (Fig. 3(c)), as common in stick systems. The direct contact between glass panels and aluminium frame is avoided providing a clearance of 5 mm. It should be noted that the silicone gaskets are attached to the internal glass layer only. Moreover, while the internal gaskets are continuous elements, the external ones are discontinuous along the panel edges (50 mm length, 250 mm spaced).

The mechanical properties were found in literature according to the classes of materials adopted by the manufacturer. In particular, for the aluminium EN-AW 6060-T6 a Young Modulus E=69 GPa was adopted, whereas for the tempered glass was adopted E=70 GPa.

A quasi-static test has been carried out increasing the force applied to the external mullion until a specific value of drift has been reached at the monitored point on the opposite mullion. Then, the force has been decreased up to zero, revealing the residual plastic deformations. Four cycles of load-unload have been performed before the failure. The force-drift cycles recorded from the load cell and the LVDT near the hydraulic jack are depicted in Fig. 5(a).

During the first cycle, a maximum displacement of 13.07 mm was attained, corresponding to a lateral force of 5.9 kN. Removing gradually the load, a residual displacement of 6.2 mm (47.7% of the cycle peak drift) has been recorded. During the second cycle the maximum displacement achieved was 32.27 mm, corresponding to a load of 11.8 kN. Removing the load, the residual displacement was 13.52 mm (41.9% of the cycle peak drift). At the third cycle the maximum displacement attained was 37.35 mm, corresponding to a lateral force of 14.7 kN. The residual displacement recorded removing the load was 14.5 mm (38.8% of the cycle peak drift).

At the fourth and last cycle, the maximum displacement achieved was 49.88 mm, corresponding to a 20.7 kN lateral force. Removing the load, the residual displacement recorded was 16.06 mm (32.2% of cycle peak drift). During the last cycles, large shear deformations involved the aluminium frame. Furthermore, residual plastic deformations between 30% and 50% of the peak displacement were recorded.

The failure was achieved during the unload phase of last cycle, when the larger glass panel fell out from its aluminium frame, due to the high deformation of the

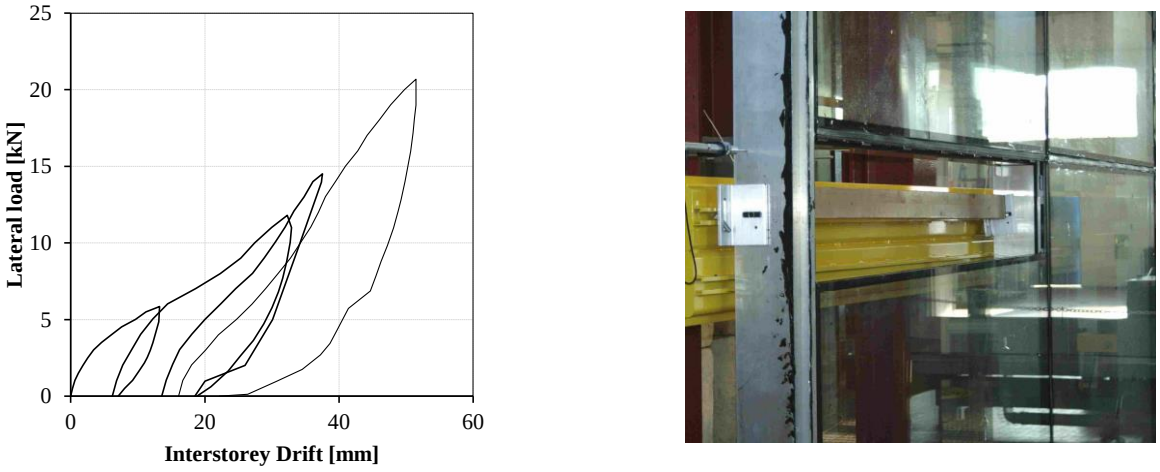

(a) (b)

Fig. 5 Façade A: force-drift cycles (a), failure mode (b)

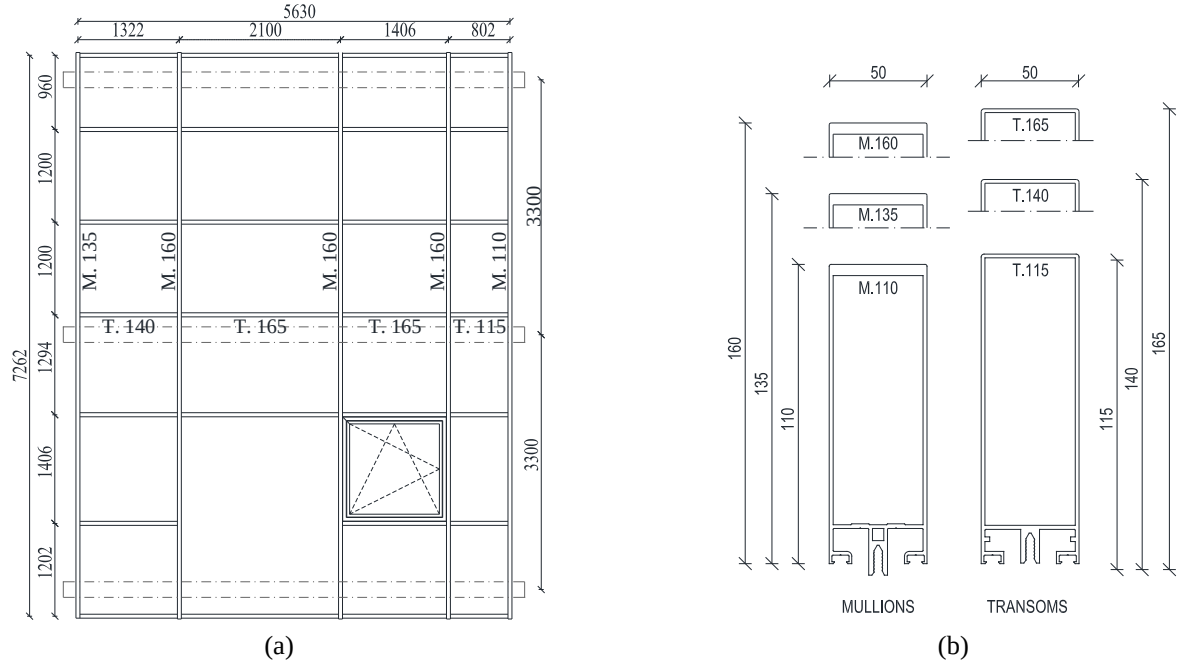

(a) (b)

Fig. 6 Façade *B*: geometry (a) and transom/mullion cross-sections (b), dimensions in mm

inferior transom (Fig. 5(b)). The specimen drift capacity was thus 49.88 mm, which corresponds to 1.6% of the interstorey height (3,100 mm). It is worth noting that this comply with the code provisions described in the section 2.

3.3 Façade B: description of the specimen, experimental activity and results

The second façade analysed is 7,200 mm high and 5,600 mm wide, with 3,300 mm interstorey height. Differently from the previous specimen, the test unit B has five mullions and six transoms (Fig. 6(a)). Three different profiles have been used for mullions, so as for transoms (Fig. 6(b)). In particular, it should be noted that transoms of the side spans are characterized by cross-section with lower inertia respect to central spans. The insulated glazing panels thickness is 8+8.2+16+6 mm, linearly supported on the edges trough silicone gaskets. Also in this specimen, just one glass panel could be opened.

In façade B, the transom-to-mullion connection is realized by using a U-shaped steel joint, which is connected to both mullion and transom by four steel screws only (Fig. 7(a)). This kind of connection results to be less stiff, especially regards relative rotation, since the latter is contrasted by screws only that act onto the thin (highly deformable) walls of the aluminium profiles connected, so allowing rotations even under moderate loads.

The glass-to-frame connection for façade B is obtained adopting silicone gaskets linearly distributed along the panels edges, see Fig. 7(b). The gaskets are continuous along the panel edges and distributed both on internal and external glass layers. The clearance between glass panels

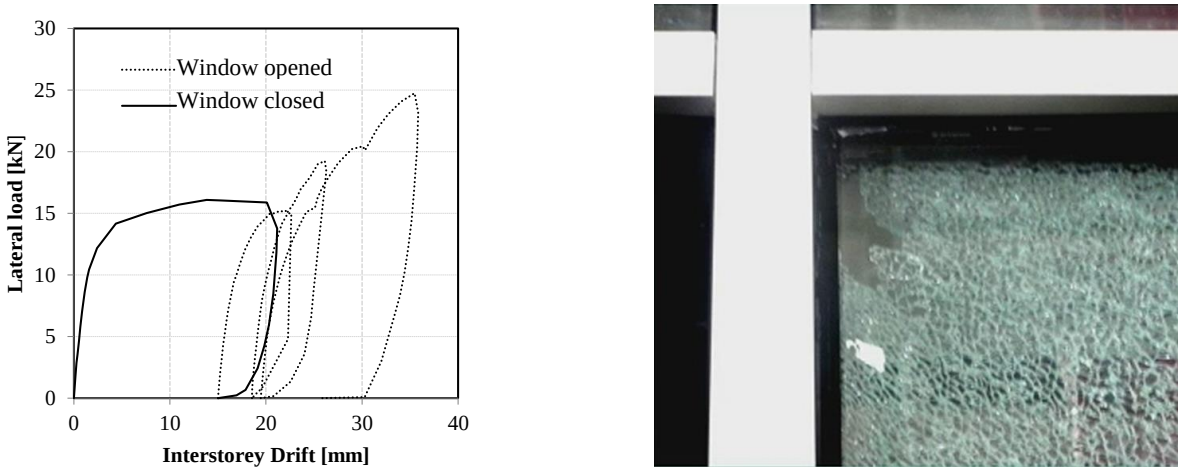

(a) (b)

Fig. 8 Façade *B*: geometry (a) and transom/mullion cross-sections (b), dimensions in mm

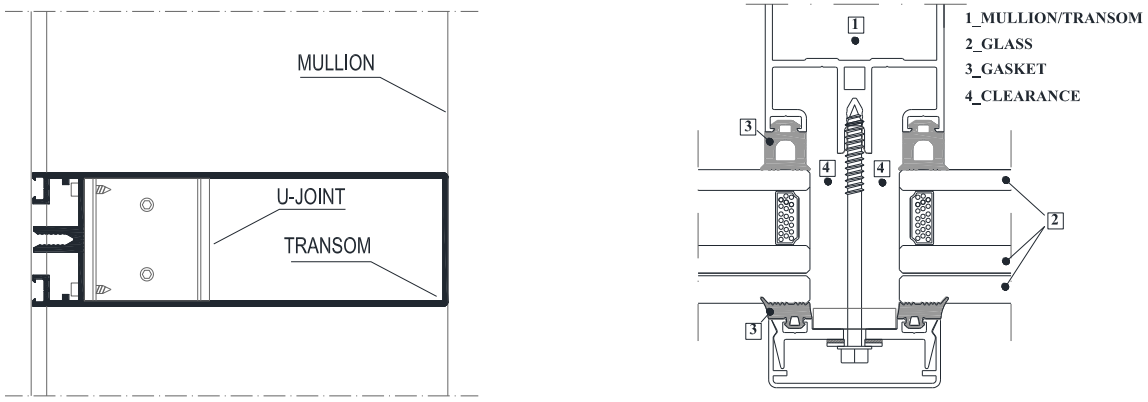

(a) (b)

Fig. 7 Façade B: Transom-to-mullion (a) and glass-to-frame (b) connections

and frame is 5 mm.

Since the specimen had an openable window, the test was performed first on the façade with closed window (first cycle) and then on the specimen with opened window (subsequent cycles), since it was impossible to reclose it due to the high shear deformations of the aluminium frame. The force-drift cycles recorded are reported in Fig. 8(a). During the first cycle (i.e., specimen with closed window), the maximum displacement achieved was 21.18 mm, corresponding to a lateral load between 15.9 kN and 16.09 kN. Removing the load, a residual displacement equal to 15.02 mm (70.9% of the peak value of drift) has been recorded.

The first cycle has been repeated on the specimen with opened window, in order to evaluate the incidence of a single glass panel on the façade global response. A lateral force of 15.9 kN was imposed to the specimen and the displacement attained was 22.64 mm. The curve stiffness is similar to that of first cycle, so the missing glass panel did not modify the façade behaviour. However, removing the load, the internal layer (thickness 6 mm) of the larger glass panel cracked at the upper corner (Fig. 8(b)), probably due to the redistribution of strength caused by the missing glass panel. A residual displacement equal to 18.54 mm has been recorded. Then, other two cycles were performed at maximum displacements of 26.29 mm and 35.86 mm. The peak forces achieved were 19.25 kN and 23.48 kN, respectively. No glass fall out has been recorded up to a maximum displacement of 35.86 mm, which corresponds to 1.08% of the interstorey height (3,300 mm). It is worth noting that this comply with the code provisions described in the section 2.

4. Finite element modelling of curtain wall stick systems

In order to predict the seismic behaviour of the stick curtain walls experimentally tested, a numerical model has been developed for each one.

The aluminium frames have been modelled using “beam” elements whereas the glass panels were modelled as “shell” elements. The transoms and mullions cross-sections have been modelled using the tool “Section Designer”, so as to reproduce the real shape of the extruded aluminium profiles. The glass shells thickness is assumed to be the sum of the single layers of the insulated system.

The principal structure beams/slabs have been modelled

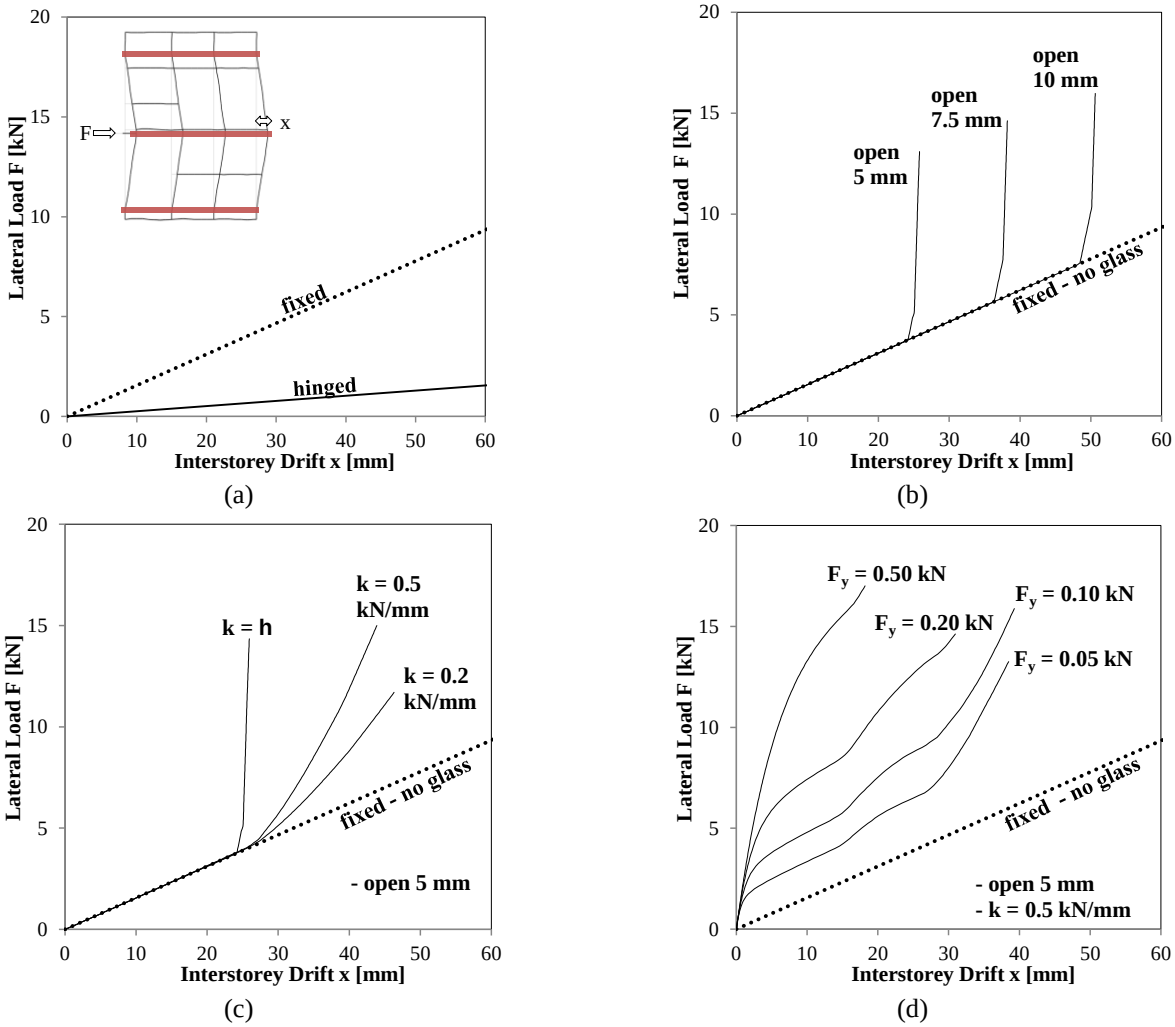

Fig. 9 Effect of transom-to-mullion connection stiffness (a), effect of clearance between glass panels and frame (b), effect of local stiffness in the glass-to-frame impact (c), effect of gasket yield force (d) on lateral response

inserting "rod" constraints between the mullions connected to the same beam/slab. Indeed, the rod constraint forces the connected points to have the same horizontal displacement during the entire loading phase.

The curtain walls response has been obtained performing non-linear static (pushover) analyses in force control. An increasing horizontal force, *F*, has been applied to the mullion at the connection with the intermediate beam of the principal structure and the interstorey drift, *x*, has been recorded.

To develop an accurate numerical model, the aluminium frame deformability, the interaction between glass panels and aluminium frame and the gasket friction were taken into account, as specified in detail in the following. In particular, four components have been recognized as main responsible of the lateral response for the analysed façades: (*i*) the aluminium frame and the rotational stiffness of transom-to-mullion connections; (*ii*) the clearance between glass panels and aluminium frame; (*iii*) the frame local stiffness in the interaction between glass and aluminium and (*iv*) the mechanical behavior of gaskets.

The shear buckling mechanism for glass panels have not been taken into account, also because such failure mode did not occur during the tests. However, in the future an enhancement of the FE model could be done as suggested by Bedona and Amadio (2016), who also take into account the effects of possible initial geometrical imperfections (i.e., non-ideal restraints), damage in glass or failure mechanisms in the restraints.

The role of each component on the overall lateral response has been examined by considering four different models (see Fig. 9), more and more complete, and herein discussed. This step-by-step investigation has been made with reference to the façade A only, since addressed to understand general concepts.

4.1 Aluminium frame and rotational stiffness of transom-to-mullion connections

In the numerical model, the aluminium frame overall behavior is linear elastic (Fig. 9(a)), where the stiffness is a function of the geometry of the façade, of the elements cross-sections and last but not least of the transom-to-mullion connections deformability.

As aforementioned, the mullions are continuous elements along the entire façade height, whereas the

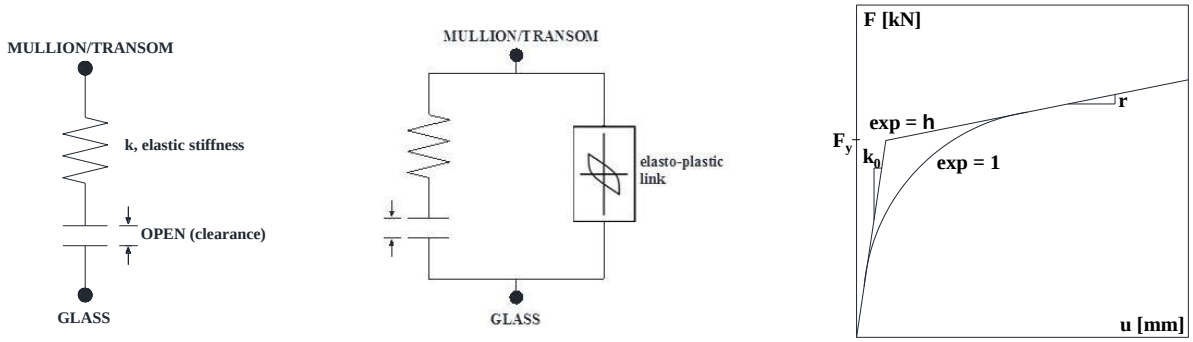

(a) (b) (c)

Fig. 10 Non-linear links: gap element (a), gap element in parallel with plastic Wen element (b), plastic Wen mathematical model (c)

Table 2 Four numerical models (Fig. 10) described through the involved components

Model	Aluminium frame	Glass	Local stiffness of the glass-to-frame impact	Gasket
(a)	✓	-	-	-
(b)	✓	✓	-	-
(c)	✓	✓	✓	-
(d)	✓	✓	✓	✓

transoms are supported between the mullions. Based on transom-to-mullion connections deformability, fixed or hinged constrains can be used for modelling the transom-to-mullion connections mechanical behaviour, see Fig. 9(a).

4.2 Clearance between glass panels and aluminium frame

To make a realistic prediction of the glass contribution to the curtain wall stiffness, the connections between glass and aluminium frame were modelled. As observed before, in stick wall systems the glass panels and the frame are not directly connected and their connection is obtained by using gaskets distributed along the glass panels edges.

The glass shells have been modelled with 200÷150 mm square meshes. Each external vertex of the mesh is connected to the mullion/transom using "gap" elements in SAP2000 (Fig. 10(a)). The gap is a non-linear link which works in compression only, and only when the clearance given by connected parts become zero. This two-nodes link simulates the clearance between glass panel and aluminium frame. When the link is "closed", the glass-to-frame contact happens and the glass participates to the global stiffness. Before the gap closure, the glass panel is free to move as a rigid body, because the rotation on the façade plane is free, as observed by Sucuoğlu and Vallabhan (1997). The contact between glass and frame is initially assumed perfectly rigid, so the elastic stiffness k assigned to the gap is assumed to be quite large.

The pushover curves for a gap open of 5-7.5-10 mm are shown in Fig. 9(b) for the fixed case (i.e., frame with fixed transom-to-mullion connections). It is worth noting that both curves coincide with the curve given by the frame only until the gap closure, as expected. After this moment, the glass panels are in contact with the frame and a sudden stiffness increase is observed.

4.3 Frame local stiffness in the interaction between glass and frame

The sudden increase of stiffness due to the glass-to-frame contact observed in the numerical curves in Fig. 8(b) appears unrealistic and far from the load-displacement curves experimentally obtained (Figs. 5, 8). These results are mainly related to the assumption about the rigid interaction between glass and frame after the closure of the clearance (i.e., gap elastic stiffness $k=\infty$). Indeed, under the action exerted by the glass panels, the aluminium thin walls of the elements in contact develop local deformations. Given the above remarks, such kind of phenomenon cannot be neglected. Instead of explicitly modelling the possibility for the aluminium cross-sections to be locally deformed, that would require the removal of the usual assumption in structural analysis about the invariance of the cross-section shape in its plane, the above behaviour can be modelled modifying the elastic stiffness of the gaps, assuming for it a finite value, rather than infinite.

Pushover curves for varying values of gap elastic stiffness, k, are shown in Fig. 9(c) for the fixed case with 5 mm gap opening. After the gap closure, the glass panels interact with the frame, contributing to the global stiffness but also locally deforming the aluminium frame. The stiffness increases slowly after the glass-to-frame impact and more similarly to the experimental evidences.

4.4 Mechanical behaviour of gaskets

Elastomeric gaskets are usually adopted for connecting glass panels to the aluminium frame. These elements, during the loading phase, are mainly subjected to shear deformations. The friction at the interface between glass and gaskets takes part to the global stiffness up to the detachment of the gaskets due to the high shear deformations. For cyclic response of façades under seismic actions, also damping due to gaskets may play a significant role. Antolinc, Žarnic *et al.* (2012, 2013), Antolinc, Rajčić *et al.* (2014) experimentally show that friction between glass panels and frame (wooden frame, in those cases) can

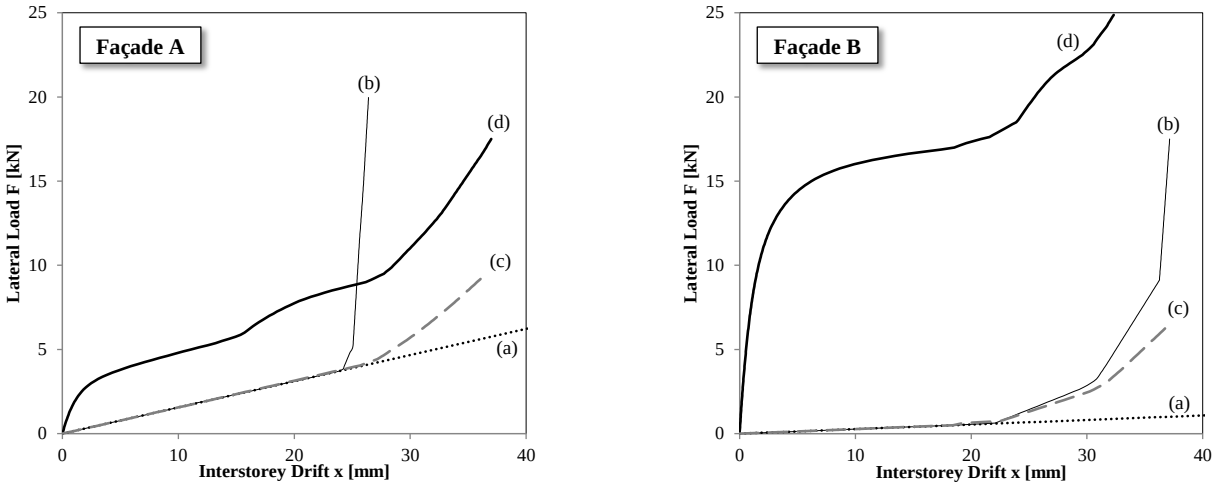

Fig. 11 Force-drift curves from different models, see Table 2: façade A (a) and façade B (b)

drastically reduce glass damage under cyclic lateral loads.

The gaskets mechanical behaviour has been modelled by inserting non-linear links which work in parallel with the aforementioned gaps, see Fig. 10(b). These two-nodes links are characterized by an elastic-plastic Wen behaviour (Fig. 10(c)), governed by the following parameters: elastic stiffness, k_0, yield force, F_y, ratio of post-yield stiffness, r, and yield exponent, exp.

The force-drift relationships obtained by inserting the gasket-to-glass friction in the model with fixed transom-to-mullion connections, gap open 5 mm and gap elastic stiffness k=0.5 kN/mm are reported in Fig. 9(d). In particular, only the effect of the yield force, F_y, on the global response is depicted, whereas the other parameters which characterize the model are set to the "optimum" values found for façade A, as indicated in next section. The effect of the gasket friction acts in the first branch of the force-drift relationships, increasing both initial stiffness and strength. For high displacement, the gasket detachment happens and the gaskets contribution to the global response became null. The gasket yield force, F_y, influences the global strength increase.

5. Finite element models for facades A and B. Numerical vs. experimental results.

In the previous section, the main phenomena which contribute to the lateral response of a generic stick curtain wall have been analysed and modelled. In particular, the contribution of aluminium frame, gasket-to-glass friction and glass-to-frame contact are now clearly defined in the load-displacement relationship. Nevertheless, the deformability of the frame members as well as the gasket-to-glass friction could not be easily predicted. By this, the properties of gaps and plastic Wen links should be derived from the experimental evidence.

In this section, four numerical models have been developed for both façade A and B, investigating all the parameters discussed before and trying to catch the experimental envelope curves, see Fig. 11(a) and (b) respectively. The phenomena taken into account in each model are also summarized in Table 2. In particular, the gap elastic stiffness and the plastic Wen initial stiffness and yield force have been calibrated in order to best matching the experimental response.

The curves (a) represent the contribution of frame aluminium only to the façade lateral response. As aforementioned, the curves elastic stiffness is a function of geometrical properties and transom-to-mullion connection stiffness. Façade A is characterized by very stiff transom-to-mullion connections, so fixed constrains have been used in the model. On the contrary, hinges were more suitable for modelling the deformability of transom-to-mullion connections of façade B.

Then, the glass panels have been inserted in the models and perfectly rigid (k=∞) gap links with an opening gap equal to 5 mm were used for modelling the glass-to-frame interaction for both façade A and B, see Fig. 11 (a) and (b), respectively - curves (b). The open value should be assumed equal to the effective clearance observed between glass panel and aluminium frame. A total of 419 and 676 gap links have been inserted in the models for façade A and B respectively.

Another case has been generated considering a finite value for the gap stiffness, k, according to the remarks made in the previous section. Curves (c) show the results for the models, where the elastic stiffness has been assumed k=0.5 kN/mm for façade A and k=5 kN/mm for façade B. As expected, the finite value of k leads to a smoother increase of the global lateral stiffness from the moment when the contact glass/frame happens on.

The last curves (d) are generated inserting also the gasket-to-glass friction in the models, through elastic-plastic Wen links. The number of links is the same of the gap inserted before, since they work in parallel. In particular, for modelling the silicone gaskets mechanical behaviour, the yield exponent has been assumed equal to 1 and the post-yield stiffness has been neglected, so null post-yield stiffness ratio. The elastic stiffness and yield force of

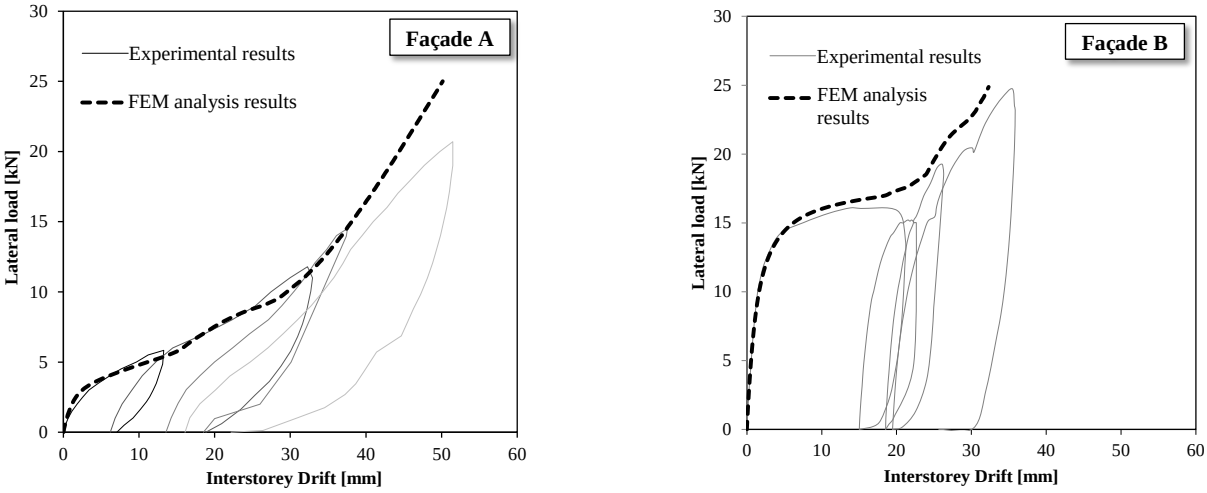

(a) (b)

Fig. 12 Comparison between experimental and numerical results: façade A (a) and façade B (b)

Table 3 Characteristics and link properties for the models adopted for Façade A and Façade B

		Façade A	**Façade B**
Transom-to-mullion rotational connection		Rigid (fixed)	Flexible (hinged)
Number of links adopted		419	676
Glass-to-frame clearance		5 mm	5 mm
Local stiffness involved in the glass-to-frame impact		0.5 kN/mm	5 kN/mm
Gasket (Wen model)	Elastic stiffness	0.7 kN/mm	7 kN/mm
	Yield force	0.1 kN	0.5 kN
	Post-yield stiffness ratio	0	0
	Yield exponent	1	1

links have been set to obtain the best match with experimental response. For façade A, a yield force F_y=0.1 kN and an elastic stiffness k_0=0.7 kN/mm have been selected as optimal values. Whereas, for façade B values of F_y=0.5 kN and k_0=7 kN/mm have been selected.

The comparison between the capacity curves (c) and (b) highlights that the gasket-to-glass friction leads to an increased initial strength and stiffness. When the behaviour of the gaskets become plastic (i.e., detachment of gaskets), the stiffness (slope) of curve (d) is reduced and becomes equal to the stiffness of the curve without friction (c). Then, when the contact between glass and frame happens, the stiffness increases suddenly in both curves (c) and (d). Then, the effects of gaskets friction is recognized as an increase of initial stiffness and a non-linear force-drift relationships until the gasket detachment. After the gasket detachment, the force-drift stiffness is governed by the aluminium frame only, since the glass-to-frame contact has still to happen. When the first gap closure is recorded, the glass panels start to participate to the global stiffness.

The links properties derived from the calibration of the numerical models on the experimental evidences are also reported and compared in Table 3. It should be noted that the two façades have shown very different behaviours, both in terms of aluminium frame and gaskets response. The frame of façade B appeared less stiff with respect to façade A, due to the different geometric asset, to the smaller profiles cross-section and especially to the lower transom-to-mullion connection rotational stiffness. On the contrary, the local stiffness after the glass-to-frame impact resulted higher for façade B if compared with façade A, due to the thicker glass.

However, the silicon gaskets have a fundamental role in the different responses of the two test units analysed. The mechanical behaviour of the silicone gaskets in terms of force-displacement relationship presents the same trend for both façades. Indeed, the post-yield stiffness ratio has been set to 0 and the yield exponent equal to 1 in both models. Nevertheless, the gaskets effect provides a considerably high initial stiffness and strength for façade B. Indeed the link elastic stiffness assumed for best matching the façade A experimental response is ten times lower than that assumed for façade B and the yield force is 0.2 times the force used for façade B. These results are probably related to the discontinuous distribution of gaskets along the glass panel edges observed in façade A and to the placement onto the internal glass layer only.

The numerical and experimental force-drift relationships for façade A and B are depicted in Fig. 12(a) and (b), respectively. The comparison between the calibrated FEM analysis and the experimental results shows a good match between the numerical models and the experimental curves for both the specimens analysed. It should be noted that response of very different curtain walls could be reliably

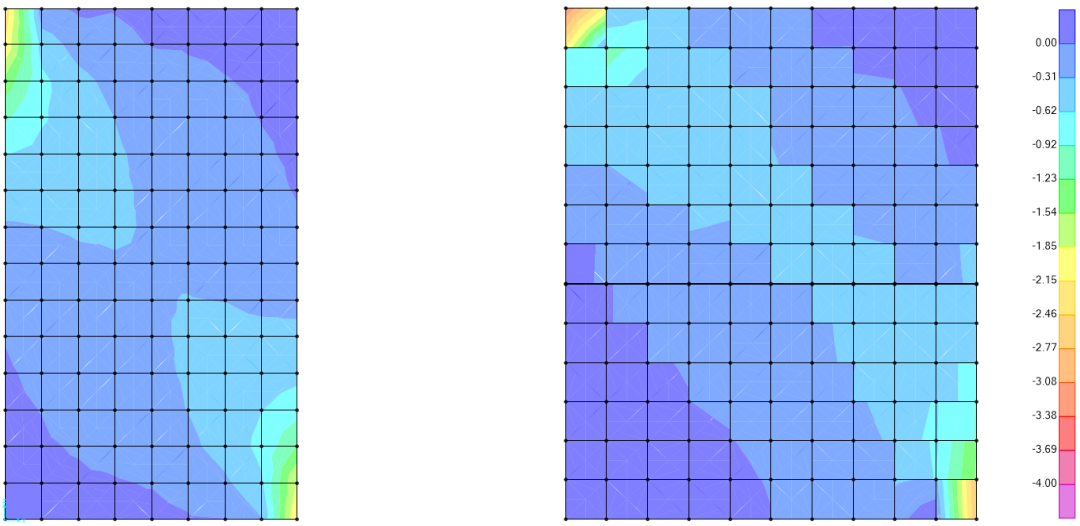

(a) (b)

Fig. 13 Stress distribution at the last step of pushover (MPa): façade A (a) and façade B (b)

predicted.

In the last instance, the glass panels stress distribution was then investigated. In particular, a stress concentration was expected at the panels corners, with maximum values achieved for the larger panels which are the first to interact with the aluminium frame due to rigid body rotation. The numerical model confirmed the stress concentration distribution, as reported in Fig. 13 for the larger panel of façade A and B at the last step of pushover analysis. The compressive strut along the main diagonal is clearly recognisable, with compressive stress concentration at corners. Compressive stresses achieved in the models are quite low (<4 MPa) if compared to the typical glass design strength range (20 ÷ 75 MPa). Tensile stresses (<1 MPa), on the other hand, are negligible if compared to the corresponding strength (greater than 45 MPa). From this perspective, the failure experimentally observed and shown in Fig. 8(b) for façade B cannot be explained. Furthermore, in both cases, failure of the glass happened in the unloading phase. This probably is because, as long as the frame is "tight" around the glass, the confinement effect and the aluminum-glass composite action somehow preserve the stability of the glass panel.

6. Conclusions

The present work aimed to investigate the behavior of stick curtain wall systems subjected to lateral loads.

The two specimens had same mechanical properties but a different geometric asset. The responses of the two test units analysed showed a similar general trend in the force-interstorey drift relationships. In particular, the force-drift curves presented an initial non-linear behavior with decreasing stiffness and a sudden stiffness increase up to the glass failure. However, the strength/deformation capacity of the two specimens are not comparable, due to the lateral response high dependence from the geometric assets.

Both specimens were designed without any care to the seismic behaviour. However, both seems to experimentally comply with the code provisions described in the previous section 2.

The lateral response of stick curtain walls has been analysed by means of finite element modelling. In particular, the effect of aluminium frame and transom-to-mullion connection stiffness, clearance between glass panels and frame, local stiffness in the glass-to-frame interaction and gasket-to-glass friction have been discussed and properly modelled. It has been found the initial force-drift curve stiffness is given by the gasket-to-glass friction, until the gasket detachment due to high shear deformations. Then, the curtain wall stiffness is related to the aluminium frame stiffness, which is a function of the transom-to-mullion connections rotational stiffness. The glass panels participate to the global lateral stiffness only after the clearance closure due to the panels rigid body motion. Moreover, the glass-to-frame impact produces plastic deformations of the transoms/mullions, which reduces the global lateral stiffness.

The study confirmed the good agreement between numerical and experimental results and the reliability of using such general method for predicting the response of stick curtain wall systems.

Further developments of this research will concern:

- the adoption of a more refined non-linear mechanical model for glass;
- the investigation of a possible procedure to assist the definition of the numerical model non-linear properties as a function of curtain walls geometrical and technological assets, even without having the experimental behavior as benchmark;
- a comprehensive analysis on further mainstream assets widely adopted for stick curtain walls;
- the analysis of the response of stick curtain walls when tested under displacement (rather than force) control and by means of hydraulic seismic actuators installed at the three levels of the setup. These actuators represent an

enhancement of the testing machine, designed to be realized in the near future. Moving horizontally each of the three levels, also asynchronously, this new setup will allow simulating the vibration of the structural frame the façade is connected to.

Acknowledgments

The work behind this paper has been done in the framework of the RELUIS research project with a grant by the Protezione Civile (Italian Emergency Agency), the METROPOLIS research project, whose implementing party is the Italian consortium Stress scarl, and the local research project at the University of Naples "Parthenope", according to the call "Support for Individual Research for the 2015-17 Period" issued by Rectoral Decree no. 727/2015.

References

American Architectural Manufacturers association (AAMA) (2001), *Recommended Dynamic Test Method for Determining the Seismic Drift Causing Glass Fallout from a Wall System*, AAMA 501.6-01.

Antolinc, D., Žarnic, R., Cepon, F., Rajcic, V. and Stepinac, M. (2012), "Laminated glass panels in combination with timber frame as a shear wall in earthquake resistant building design", *Challenging Glass 3: Conference on Architectural and Structural Applications of Glass*, CGC 2012, 623-631.

Antolinc, D., Žarni, R., Stepinać, M., Rajčič, V., Krstevska, L. and Tashkov, L. (2013), "Simulation of earthquake load imposed on timber-glass composite shear wall panel", *Proceedings COST Action TU0905 Mid-Term Conference on Structural Glass*, 245-252.

Antolinc, D., Rajčić, V. and Žarnić, R. (2014), "Analysis of hysteretic response of glass infilled wooden frames", *J. Civil Eng. Manage.*, **20**(4), 600-608.

ASCE (2013), *Minimum design loads for buildings and other structures*, ASCE 7-10, Reston, VA.

Baird, A., Palermo, A. and Pampanin, S. (2011), "Facade damage assessment of multi-storey buildings in the 2011 Christchurch earthquake", *Bull. N.Z. Soc. Earthq. Eng.*, **44**(4), 368-376.

Bedon, C. and Amadio, C. (2016), "A unified approach for the shear buckling design of structural glass walls with non-ideal restraints", *Am. J. Eng. Appl. Sci.*, **9**(1), 64-78

Behr, R.A., Minor, J.E. and Norville, H.S. (1993), "Structural behavior of architectural laminated glass", *J. Struct. Eng.*, **119**(1), 202-222.

Behr, R.A., Belarbi, A. and Brown, A.T. (1995a), "Seismic performance of architectural glass in a storefront wall system", *Earthq. Spectra*, **11**(3), 367-391.

Behr, R.A., Belarbi, A. and Culp, J.H. (1995b), "Dynamic racking tests of curtain wall glass elements with in- plane and out- of-plane motions", *Earthq. Eng. Struct. Dyn.*, **24**(1), 1-14.

Behr, R.A. (1998), "Seismic performance of architectural glass in mid-rise curtain wall", *J. Arch. Eng.*, **4**(3), 94-98.

Bouwkamp, J. G. and Meehan, J. F. (1960), "Drift limitations imposed by glass", *Proceedings of the Second World Conference on Earthquake Engineering*, Tokyo, Japan.

Bouwkamp, J.G. (1961) "Behavior of window panels under in-plane forces", *Bull. Seismol. Soc. Am.*, **51**(1), 85-109.

Brueggeman, J.L., Behr, R.A., Wulfert, H., Memari, A.M. and Kremer, P.A. (2000), "Dynamic racking performance of an earthquake-isolated curtain wall system", *Earthq. spectra*, **16**(4), 735-756.

Carré, H. and Daudeville, L. (1999), "Load-bearing capacity of tempered structural glass", *J. Eng. Mech.*, **125**(8), 914-921.

European Standard (2003), *Eurocode 8: Design of structures for earthquake resistance. Part 1: General rules, seismic actions and rules for buildings*, EN 1998-1, Brusselles, Belgium.

Evans, D., Kennett, E., Holmes, W.T. and Ramirez, F.J.L. (1988), "Glass damage in the September 19, 1985 Mexico City earthquake", *Steven Winter Associates*.

FEMA 450 (2003), *Recommended provisions for seismic regulations for new buildings and other structures*, FEMA.

Filiatrault, A., Christopoulos, C. and Stearns, C. (2002), "Guidelines, specifications, and seismic performance characterization of nonstructural building components and equipment", *Pacific Earthquake Engineering Research Center*.

Hosseini, M. (2005), "Behavior of nonstructural elements in the 2003 Bam, Iran, earthquake", *Earthq. Spectra*, **21**(S1), 439-453.

Hutchinson, T.C., Zhang, J. and Eva, C. (2011), "Development of a drift protocol for seismic performance evaluation considering a damage index concept", *Earthq. Spectra*, **27**(4), 1049-1076.

Huveners, E. M. P., van Herwijnen, F., Soetens, F. and Hofmeyer, H. (2007), "Glass panes acting as shear wall", *Heron-English Edition*, **52**(1-2), 5.

JASS 14 (1996), *Japanese Architectural Standard Specification Curtain Wall*, AIJ, Architectural Institute of Japan.

Lim, K.Y.S. and King, A.B. (1991), "The behavior of external glazing systems under seismic in-plane racking", Building Research Association of New Zealand, BRANZ.

Memari, A.M., Behr, R.A. and Kremer, P.A. (2000), "Toward development of a predictive model for drift limits in architectural glass under seismic loadings", *Proceedings of the 12th World Conference on Earthquake Engineering*, Auckland, New Zealand.

Memari, A.M., Behr, R.A. and Kremer, P.A. (2004), "Dynamic racking crescendo tests on architectural glass fitted with anchored pet film", *J. Arch. Eng.*, **10**(1), 5-14.

Memari, A.M., Kremer, P.A. and Behr, R.A. (2006), "Architectural glass panels with rounded corners to mitigate earthquake damage", *Earthq. spectra*, **22**(1), 129-150.

Memari, A.M. and Shirazi, A. (2004), "Development of a seismic rating system for architectural glass in existing curtain walls, storefront and windows", *Proceedings of the 13th World Conference on Earthquake Engineering*, Vancouver, Canada.

Memari, A.M., Shirazi, A. and Kremer, P.A. (2007), "Static finite element analysis of architectural glass curtain walls under in-plane loads and corresponding full-scale test", *Struct. Eng. Mech.*, **25**(4), 365-382.

Memari, A.M., Shirazi, A., Kremer, P.A. and Behr, R.A. (2011), "Development of finite-element modeling approach for lateral load analysis of dry-glazed curtain walls", *J. Arch. Eng.*, **17**(1), 24-33.

O'Brien Jr, W.C., Memari, A.M., Kremer, P.A. and Behr, R.A. (2012), "Fragility Curves for Architectural Glass in Stick-Built Glazing Systems", *Earthq. Spectra*, **28**(2), 639-665.

Pantelides, C.P. and Behr, R.A. (1994), "Dynamic in- plane racking tests of curtain wall glass elements", *Earthq. Eng. Struct. Dyn.*, **23**(2), 211-228.

Pantelides, C.P., Truman, K.Z., Behr, R.A. and Belarbi, A. (1996), "Development of a loading history for seismic testing of architectural glass in a shop-front wall system", *Eng. Struct.*, **18**(12), 917-935.

SAP2000, release 17 (2014), Static and Dynamic Finite Element Analysis of Structures, Computers and Structures Inc., Berkeley, CA, USA.

Sivanerupan, S., Wilson, J.L., Gad, E.F. and Lam, N.T.K. (2009), "Seismic Assessment of Glazed Façade Systems", *Proceedings of the Annual Technical Conference of the Australian*

Earthquake Engineering Society, Newcastle, Australia.
Sucuoğlu, H. and Vallabhan, C.G. (1997), "Behaviour of window glass panels during earthquakes", *Eng. Struct.*, **19**(8), 685-694.
Thurston, S.J. and King, A.B. (1992), "Two-directional cyclic racking of corner curtain wall glazing", Building Research Association of New Zealand, BRANZ.

CC